Published in final edited form as:
Anal Chem. 2011 December 15; 83(24): 9361–9369. doi:10.1021/ac201952t.

Determining transport efficiency for the purpose of counting and sizing nanoparticles via single particle inductively coupled plasma-mass spectrometry

Heather E. Pace[1,3], **Nicola J. Rogers**[1], **Chad Jarolimek**[1], **Victoria A. Coleman**[2], **Christopher P. Higgins**[3], and **James F. Ranville**[4,*]

[1]CSIRO Land and Water, Lucas Heights, NSW 2234 Australia

[2]National Measurement Institute, Nanometrology Section, West Lindfield, NSW 2070 Australia

[3]Colorado School of Mines, Environmental Science and Engineering, Golden, CO 80401 USA

[4]Colorado School of Mines, Chemistry and Geochemistry, Golden, CO 80401 USA

Abstract

Currently there are few ideal methods for the characterization of nanoparticles in complex, environmental samples, leading to significant gaps in toxicity and exposure assessments of nanomaterials. Single particle-inductively coupled plasma-mass spectrometry (spICP-MS) is an emerging technique that can both size and count metal-containing nanoparticles. A major benefit of the spICP-MS method is its ability to characterize nanoparticles at concentrations relevant to the environment. This paper presents a practical guide on how to count and size nanoparticles using spICP-MS. Different methods are investigated for measuring transport efficiency (i.e. nebulization efficiency), an important term in the spICP-MS calculations. In addition, an alternative protocol is provided for determining particle size that broadens the applicability of the technique to all types of inorganic nanoparticles. Initial comparison, using well-characterized, monodisperse silver nanoparticles, showed the importance of having an accurate transport efficiency value when determining particle number concentration and, if using the newly presented protocol, particle size. Ultimately, the goal of this paper is to provide improvements to nanometrology by further developing this technique for the characterization of metal-containing nanoparticles.

Nanotechnology, defined as the intentional manipulation of materials at the nanometer scale[1], underpins a rapidly growing industry with applications in a wide range of commercial and private sectors. While this technology is expected to have many benefits, it is important that potential risks are identified as quickly as possible to ensure responsible use. One of the difficulties scientists have encountered in describing the toxicity of nanomaterials is that toxic effects have been shown to be complex in nature, and more than just a function of nanoparticle mass. Toxicity may be related to a number of nanoparticle properties including size, surface chemistry, aggregation state and solubility to name a few[2–6]. Characterization of nanomaterials is thus a crucial component to nanotoxicology studies for proper interpretation of the results and better correlation between nanoparticle properties and any observed toxicity.

*Fax: +1-303-273-3629. jranvill@mines.edu.

ASSOCIATED CONTENT

Supporting Information. Additional information as noted in text. This material is available free of charge via the Internet at http://pubs.acs.org.

Nanoparticle dispersions exist as dynamic, non-equilibrium systems that are highly sensitive to the chemistry of the dispersion medium as well as the physicochemical properties and concentration of the nanoparticles themselves[7]. As a result, many nanoparticle properties are not constant across different tests, different concentrations within the same test, or even over time within the same dispersion. Consequently, beyond simple characterization of the starting material, it is recommended that nanoparticles used in toxicity testing also be characterized *in situ*, over a relevant time-frame. Many of the current methods available for the characterization of nanoparticles are not suitable for environmental systems[8, 9]. One of the main challenges many techniques face when characterizing nanoparticles in environmental systems is poor method sensitivity. For instance, expected exposure concentrations of engineered nanoparticles in aqueous environments are speculated to be in the sub-μg/L range, or approximately 10^3 to 10^5 particles/mL[10, 11]. This is at least an order of magnitude lower than the method sensitivity of many characterization techniques, such as dynamic light scattering, differential centrifugal sedimentation and field flow fractionation[8]. Environmental systems also present analytical techniques with numerous interferences from the complex matrix components, such as natural particles, humic substances, and debris. As a result, investigators often have to extrapolate information from measurements made using artificially high nanoparticle concentrations in simplified systems. Consequently, improvements and/or developments in nanoparticle metrology within environmental systems are now considered to be one of the highest priorities in the assessment of nanotechnology risks[12, 13]. Single particle inductively coupled plasma-mass spectrometry (spICP-MS) is an emerging, analytical method with the potential to address some of these more crucial properties, such as particle size, aggregation state and particle number concentration, at environmentally relevant concentrations.

In a series of papers, Degueldre et al.[14–18] first presented the theory of spICP-MS for characterizing colloids in aqueous solutions. These authors provided theoretical equations for sizing and counting particles as well as demonstrating the feasibility of spICP-MS using various inorganic nanoparticles (80–250nm). Recently, Laborda et al.[19] presented work further demonstrating the potential for spICP-MS to be a useful characterization tool for nanoparticles. Beyond these studies, only a handful of other researchers have investigated single particle ICP methods[20–24]. Further development and validation is needed before spICP-MS can become a routine characterization technique in nanoparticle research.

The objective of this paper is to present a practical guide on how to quantitatively count and size nanoparticles using spICP-MS. To this end, the protocol for carrying out spICP-MS analysis, including the steps and equations needed to process the data, is described in detail. While much of this has been previously reported in the literature, this paper presents two modifications that aim to improve both the accessibility and universality of the technique. These modifications are described below.

An important omission in the previously described protocols was a clear explanation of how to determine all of the terms used in the counting and sizing equations. Specifically, both Degueldre et al.[14–18] and Laborda et al.[19] present an equation for finding particle number concentration that depends on knowing a term referred to as the nebulization efficiency, also known as (aerosol) transport efficiency in much of the traditional ICP-MS literature. However, it was unclear how this value was obtained. In the present study, different ways to measure this term are explored, including two new methods that use spICP-MS theory to directly determine transport efficiency.

Secondly, an alternative procedure for determining particle size was developed, which uses dissolved standards instead of monodisperse nanoparticles for calibration. By using dissolved standards this procedure is more easily applied to a range of inorganic

nanoparticle types. This new protocol uses transport efficiency in the calculation of particle size, further emphasizing the importance of accurately determining this term. The analysis of a well-characterized, monodisperse silver nanoparticle suspension was used to verify the accuracy of the measured transport efficiency term as well as to provide initial validation of the presented spICP-MS protocol. Subsequent work will more thoroughly validate the new sizing equations by comparing the performance characteristics of spICP-MS analysis to other commercially available particle sizing methods[25].

THEORY

Inductively coupled plasma-mass spectrometry (ICP-MS) is an analytical technique that provides rapid elemental analysis at ultratrace (ng/L) concentrations. Traditionally, ICP-MS measures total metal concentrations in samples containing dissolved metals. The ICP-MS detects metal ions based on their mass to charge ratio and assigns an intensity reading which is correlated to the amount of metal that was detected during a user-specified interval of time (i.e. dwell time with units of ms per reading or event). The intensities are then related back to a calibration curve based on standards with known metal concentration to determine the metal concentration for the sample.

In traditional ICP-MS, multiple intensity readings are integrated over long dwell times (0.3–1 s) and averaged to produce an overall metal concentration for the sample. In contrast, in spICP-MS each intensity reading is integrated over a shorter dwell time (10 ms or less) and plotted individually as a function of time. If the sample contains dissolved metals, the ions will be distributed homogenously within the solution, and the mass of metal entering the plasma per unit of time, and subsequently traveling to the detector as ions, will be relatively constant, producing a consistent intensity signal vs. time across readings. However, if the sample contains nanoparticles, the metal atoms within the sample are no longer distributed homogenously. Instead the metals are present as discrete particulates with 100's–1000's of metal atoms per particle. In this scenario, instead of a constant flow of metal ions through the instrument, single particles enter the ICP-MS plasma and, once ionized, move through the mass analyzer to the detector as a cluster of ions. This cluster of ions results in a spike in intensity above the background, where the pulse corresponds to an individual nanoparticle and the background represents the “dissolved” metals in solution (consisting of unresolved smaller nanoparticles as well as truly dissolved species).

The fundamental assumption behind spICP-MS is that each pulse represents a single particle event (i.e. a particle or aggregate), which depends on short dwell times, constant flow rate and a sufficiently low particle number concentration. If this assumption is true then the frequency of the pulses is directly related to the number concentration of particles/aggregates (particle number per volume) and the intensity of the pulse (i.e. height) is related to particle size (mass). The equations used in the present study for determining both particle number concentration and particle size by spICP-MS are shown below.

Relating pulse frequency to particle number concentration

Degueldre et al.[14–18], relates the frequency of the particle events, $f(I_p)$ (# of pulses/ms), to a particle number concentration, N_p (particles/mL), using Equation 1,

$$N_p = \frac{f(I_p)}{q_{liq} * \eta_n} \quad [1]$$

where q_{liq} (mL/ms) is the sample flow rate and η_n is the transport efficiency. If the transport efficiency is known, then Equation 1 can be used to determine particle number concentration (Figure 1).

Relating pulse height to particle size

Degueldre and colleagues[14–18] also present an equation for calculating particle size. This equation includes a term, referred to as the counting yield that has units of counts per atom. The counting yield term accounts for the losses that occur as ions are transported from the plasma, through the interface and mass analyzer, to the instrument detector. In the work presented by Degueldre et al.[17] determination of counting yield was accomplished via a particle size (or mass) versus signal intensity plot. Given different elemental ions will experience variations in the transmission efficiency from the plasma to the detector, when producing a size versus intensity plot to determine counting yield, the reference nanoparticles with pre-determined size should have the same elemental composition as the unknown sample for the most accurate determination of counting yield. For nanoparticle types where suitable reference materials exist, this method is appropriate. For other nanoparticle types, such as TiO_2 and CeO_2, acquiring such reference dispersions with guaranteed particle size is difficult because they are not always synthesized as highly monodisperse samples and tend to aggregate once in suspension. In the present study, an alternative protocol was developed where pulse height was related to particle size by using transport efficiency (this term is also used to count particles, see Eq. 1) and a traditional dissolved standard calibration curve. This protocol assumes that once past the plasma, ions from a dissolved s tandard solution and ions from a nanoparticle will behave comparably, given they are the same analyte. The transport efficiency accounts for the differences in the mass delivery of dissolved solutions versus a single nanoparticle when detected during a short dwell time. All other efficiencies, which contribute to the counting yield, are captured in the dissolved standard calibration curve. The equations for this alternative protocol are presented below (Equations 2–4).

ICP-MS is ultimately a mass-based technique where particle size is determined by relating the pulse signal intensity (I_p) to an elemental mass. As in traditional ICP-MS analysis, the first step in developing a new protocol was to create a dissolved standard calibration curve. This correlates the signal intensity from the instrument to the concentration of the analyte entering the plasma (Figure 1). The second step was to relate the concentration of the dissolved analyte to the total analyte mass that enters the plasma during each reading. The relationship between analyte concentration, C (μg/mL), and, W, the mass observed per event, (μg/event), is given in Equation 2:

$$W=[\eta_n * q_{liq} * t_{dt} * C], \quad [2]$$

where q_{liq} (mL/ms) is the sample flow rate, t_{dt} (ms/event) is the dwell time, and η_n is the transport efficiency. The resulting calibration curve relates signal intensity (counts/ event) to a total mass transported into the plasma per event. The intensity of each individual pulse, I_p (counts/event), can then be inserted into the newly transformed calibration curve to determine the mass of the corresponding particle, m_p, (Equation 3)

$$m_p = f_a^{-1} * \left[\frac{\left((I_p - I_{Bgd}) * \eta_i \right) - b}{m} \right], \quad [3]$$

where f_a is the mass fraction of the analyzed element in the particle, η_i is the particle ionization efficiency (discussed in more detail below), and m and b are the slope and y-intercept of the calibration curve (Figure 1). The average background intensity, I_{Bgd} (counts/ event), is subtracted from the pulse intensity in order to remove any contribution from dissolved species to the total pulse signal.

Assuming a spherical geometry, Equation 4 relates particle mass to diameter, *d*, where ρ is the particle density.

$$d = \sqrt[3]{\left[\frac{6 * m_p}{\pi * \rho}\right]}. \quad [4]$$

Transport efficiency

The transport efficiency is defined as the ratio of the amount of analyte entering the plasma to the amount of analyte aspirated[26]. In the calculation of particle number concentration, the use of transport efficiency is straight-forward in that it simply accounts for the volume loss during transport of the aerosolized suspension through the spray chamber. Less intuitive is the application of this efficiency in the calculation of particle size. The need for the transport efficiency term lies in the difference between the mass transport of a single nanoparticle through the nebulizer/spray chamber system as compared to that of dissolved ions in solution. Conceptually, a single particle travelling through the sample introduction section of the ICP-MS will remain intact until it enters the plasma. Consequently, the mass of metal reaching the plasma from a single particle is related to the particle size and is independent of the volume of solution that travels with the particle. In contrast, for a dissolved metal solution the total mass reaching the plasma will depend on the concentration of the metal and the volume of the solution that travels through the spray chamber to the plasma during a set dwell time. To convert pulse intensity to particle mass using a dissolved metal calibration curve, the transport efficiency, is needed to relate concentration of the metal standard to a total mass flux. This effectively converts the dissolved metal calibration curve from intensity versus concentration to intensity versus mass observed per event (i.e. reading). Then, using this new calibration curve, the pulse intensity can be converted to a particle mass.

Given the above discussion, it is clear that an accurate transport efficiency value is crucial for the success of spICP-MS as a quantitative technique. Reported values in the literature typically range from 1 to 5%[27–29], but can be much higher for high-efficiency nebulizer systems[30, 31]. These values have been shown to depend not only on the components of the sample introduction system (i.e. nebulizer, spray chamber), but also on various operational parameters, such as gas flow, sample viscosity and uptake rates[27, 28, 32]. This means that across different instruments, operational set-ups, and sample types the transport efficiency can vary. In other words, the transport efficiency is instrument specific, and thus, needs to be measured on a regular basis for accurate sizing and counting results. It is likely that under the same operational and sample conditions, using the same instrument, the transport efficiency will not vary significantly from day to day, nevertheless, in the present study, it was measured regularly to ensure the most accurate results.

Particle behavior in an ICP-MS

When using dissolved metal standards as a mass calibration for particle dispersions it is important to consider under what conditions particles behave differently from ions in solution while traveling through the ICP-MS. Fortunately, the analysis of particulate samples by ICP-MS is not a new concept. For decades, researchers in the area of slurry nebulization have been developing methods for the analysis of particulates by ICP-MS as a way to measure total metals directly from solids[33, 34]. Findings from this research show that the analyte recovery from slurries (i.e. particle dispersions) is highly dependent on particle size and total solids concentration. The size and concentration of particles were thought to affect two processes in the ICP-MS, the transport efficiency of the particles from the sample introduction system (i.e. nebulizer/spray chamber) to the plasma, and the efficiency of the plasma to ablate, atomize, and ionize particulate metals[33]. Regarding transport efficiency,

most researchers have found that particles larger than 2–5 μm may be selectively removed in the spray chamber[35–37]. This means that the upper size limit for particle characterization by spICP-MS is around 2 μm, which is sufficient for nanoparticles and small aggregates, but may omit larger aggregates from analysis. Besides the influence of particle size, slurry nebulization research has shown that high solids content (0.1–1% w/v) can affect transport efficiency by changing the nebulization process[29, 38]. Given that total particle concentrations for spICP-MS analysis are necessarily far below 0.1% w/v solids in order to avoid coincidence, this is not a major concern.

For plasma ionization efficiency, research shows that as long as the above parameters are met for particle size and total concentration, generally the plasma ionizes particulates with a similar efficiency to the corresponding dissolved species[35, 36]. If this is the case, then the particle ionization efficiency, η_i, defined as the ratio of the ionization efficiency of the particle to the ionization efficiency of the corresponding dissolved metal solution, is considered to be 100%. Specifically, for both silver and gold nanoparticles the ionization efficiency has been investigated and shown to be 100% for the size ranges used in the present study[19, 20]. Thus, η_i=100% was used in all calculations. Different engineered nanoparticles could have varying degrees of recalcitrance towards full particle ablation and ionization, which affects the particle ionization efficiency. Therefore, it is important to determine this before attempting to size nanoparticles of different composition. One way to measure ionization efficiency for the nanoparticles of interest is to compare total metal concentration of digested (i.e. dissolved) nanoparticles and undigested nanoparticles. If the ratio of these two concentrations is significantly lower than 1, then the pulse signal from the particle can be adjusted accordingly by inputting that ratio into Equation 3. However, if the particle ionization efficiency is severely reduced for certain nanoparticle types it is likely that the ionization efficiency could vary greatly with increasing particle size. If this happens, then the direct relationship between pulse height and particle size will start to degrade, and the sizing of these particles may no longer be possible. Overall, slurry nebulization research suggests that analysis of nanoparticles by spICP-MS can use dissolved standards for calibration.

EXPERIMENTAL SECTION

spICP-MS analysis

A quadrapole ICP-MS with a Micromist nebulizer and a Scott Double Pass spray chamber (Agilent 7500 CE, Agilent Technologies, CA, USA) was used for single particle analysis of the nanoparticle samples. The data acquisition for the instrument was set to time-resolved analysis (TRA) mode, thus collecting intensities as a function of time (i.e. counts/dwell-time interval). The measurement duration of each run was 30 s with a data acquisition rate, or dwell time, of 10 ms/event. At the beginning of each run the instrument was tuned using a multi-element tune solution for optimal sensitivity and minimum oxide and double-charged species levels (Table S-1, Supporting Information). The tune solution was made in-house using 1 μg/L Li, Co. Y, Tl, Ce, and Ba in 1% v/v hydrochloric acid (Merck, Darmstadt, Germany). A calibration curve was produced using dissolved standards (AccuTrace, CT, USA) prepared in 0.2% trace pure nitric acid (Merck, Darmstadt, Germany). The peristaltic pump was set to 0.05 rps for all experiments, which translates to a sample flow rate of approximately 0.18 mL/min. However, given the potential for slight day to day differences, the flow rate was measured during each experiment. Due to the rapid data sampling rate, only one isotope (^{107}Ag for silver and ^{197}Au for gold) was monitored during analysis. Data, in the form of counts per dwell-time interval as a function of time, were exported to a spreadsheet for further processing.

Data processing for spICP-MS

The first step for determining a particle size distribution and number concentration from spICP-MS analysis is to separate the particle events (i.e. the pulses) from the background signal. Following an established procedure[17, 19, 20], the process used in the present study for determining particle events starts by averaging the entire dataset and collecting all data points that are three standard deviations (3σ) above the mean of the entire dataset. This is similar to the removal of outliers from a normally distributed data set, and it is assumed that the background data points have a (near) normal distribution. The remaining data set is then re-averaged and the standard deviation re-calculated, and again all data points 3σ above the new mean are collected. This process is repeated until there are no more data points 3σ above the final mean. The remaining data set represents the background signal, and the collection of data points that were removed from the dataset across all iterations are the particle events. Following separation of particles from the background signal, the number of particle events per scan can then be related back to a particle number concentration, and the intensity of each individual particle event (counts per dwell-time interval) can then be used to determine a particle size (Figure 1). A particle size distribution can then be constructed by binning the individual particle events by size and plotting the resulting histogram.

Determination of transport efficiency

In the present study, the transport efficiency was measured using three separate methods (Table 1). The first method, referred to as the waste collection method, determines transport efficiency indirectly via collection of the waste stream exiting the spray chamber and determining the total analyte going to the plasma by comparing the waste volume to the sample uptake volume[27, 28, 39, 40]. For this study the specific procedure was adapted from that of Gustavsson[40]. The waste collection method was conducted with the plasma ignited and the instrument set to the same parameters as those determined during that day's instrument tune. A vial with 50–100 mL dissolved gold solution and an empty waste vial with attached waste tubing were both weighed before analysis. Prior to placing the sipper into the sample vial, the ICP-MS introduction system was quickly flushed with air to remove any residual solution. Flushing continued until liquid no longer came out into the waste tubing. The peristaltic pump was stopped and the empty waste vial with attached tubing was connected to the spray chamber. The sipper was placed into the sample vial and the pump started. After 60 minutes the sipper was removed from the sample vial and placed into a clean, empty vial. The pump was allowed to continue at its current speed until solution was no longer coming out of the spray chamber into the waste tubing. The system was again rapidly flushed with air to clear out any remaining solution caught in the spray chamber. The waste tubing was carefully removed from the spray chamber and both tubing and waste vial were weighed. Transport efficiency was calculated by dividing total volume of sample aspirated (i.e. weight difference of sample vial before and after analysis) by the volume difference between the sample uptake and waste stream (i.e. total weight difference of sample and waste vials plus tubing before and after analysis).

Previous literature has also described direct methods for determining transport efficiency that measure the aerosol exiting the spray chamber on its way to the plasma[28]. These methods are typically conducted with the plasma off and require the addition of some sort of device (e.g. glass filter) placed in between the spray chamber and the plasma that captures/measures the aerosol. While these direct methods for measuring transport efficiency have been shown to be more accurate than their indirect counterparts, the need for specialized equipment and an involved instrument set-up was seen as a significant drawback. Considering these limitations, direct methods as described in the literature were not explored in this study.

The second and third methods used here have not been previously described, but in principle, are similar to direct methods in that they measure what has actually entered the plasma. Instead of requiring specialized equipment, both methods rely on a well-characterized reference nanoparticle sample and the theory of spICP-MS to determine the transport efficiency. Specifically, the second method, referred to as the particle size method, measures transport efficiency by using reference nanoparticles of known particle size. The third method, referred to as the particle frequency method, uses a reference nanoparticle suspension of known particle number concentration to find transport efficiency. For both methods, the 60nm gold reference nanoparticles from the US National Institute of Standards and Technology (NIST, RM 8013) were used. An assessment of the sensitivity of two methods to the either the measure average particle size or the total gold concentration is presented in Supplemental Information.

Similar to Degueldre and colleagues[14–18], the first step of the particle size method is to create a calibration curve using monodisperse nanoparticles that relates intensity to particle mass. Assuming only one particle enters the plasma per dwell-time interval; the mass flux into the plasma per reading is the mass of a single nanoparticle. With a known particle size, d, and density, ρ, the particle mass, m_p, can be calculated using Equation 5.

$$m_P = \frac{\pi d^3}{6} * \rho. \quad [5]$$

If the diameter used in Equation 5 is the average diameter of a monodisperse particle suspension, then the most common pulse intensity (i.e. the peak position of the raw data histogram) should represent the intensity that corresponds to the mass of the average sized particle. To accurately find the peak intensity from the binned raw data, a Gaussian curve was fitted to the histogram using OriginPro 8.5.1. Subsequently, the peak position of one or more reference nanoparticle materials can then be plotted against the average particle mass to create a calibration curve relating intensity to mass per event. In our case, only one reference nanoparticle material was used, so the average intensity of a blank, with a mass delivery of 0 μg/event, was also included to create a two-point calibration curve with the following linear regression equation (Equation 6),

$$Y = \mathrm{m}_{\mathrm{NP}}(W) + \mathrm{b} \quad [6]$$

where Y is the instrument response (counts/10ms), W is the mass per event (μg/event), b is the signal of the instrumental background noise, and m_{NP} is the linear slope of the resulting calibration curve.

The second, concurrent step of the particle size method is to create a corresponding dissolved calibration curve. In our case it was a dissolved gold calibration curve. Then, by multiplying each dissolved standard concentration by the sample flow rate and the dwell time, the total mass entering the sample introduction system for each event can be calculated. This is essentially Equation 2 without the transport efficiency, which means the losses that occur in the spray chamber have yet to be taken into account. In other words, each mass value in the dissolved calibration curve needs to be multiplied by the transport efficiency to obtain the correct mass flux into the plasma. This can be written mathematically by dividing the slope from the dissolved calibration curve by the transport efficiency (Equation 7),

$$Y = \frac{m_{\mathrm{diss}}}{\eta_n} (W_{diss}) + \mathrm{b} \quad [7]$$

where Y is the instrument response, W_{diss} is the mass delivery of dissolved metals per dwell-time interval, η_n is the transport efficiency, b is the signal of the instrumental background noise, and m_{diss} is the slope of the calibration curve.

Assuming equal transport efficiencies between particulate and dissolved solutions and given the ionization efficiency of the reference nanoparticle(s) is 100%, Equations 6 and 7 should be equivalent. Thus, by setting the two slopes equal, the transport efficiency is found to be the ratio of m_{diss} to m_{NP}.

In the third method, transport efficiency is determined by measuring the pulse frequency (pulses/s) of a nanoparticle suspension with a known particle number concentration. In this study, the particle number concentration of the 60nm gold nanoparticle stock suspension was calculated from the total gold concentration and from the nanoparticle diameter, which were 51.86 mg/L Au and 55 nm respectively[41]. The stock solution was then diluted using MilliQ water (18.2 MΩ, filtered through 0.22 μm). With a known particle number concentration, N_P, the sample flow rate, q_{liq}, and the measured pulse frequency, $f(I_p)$, the transport efficiency was found using Equation 8 (Equation 1 rearranged).

$$\eta_n = \frac{f(I_p)}{q_{liq} * N_p}. \quad [8]$$

Nanoparticle suspensions

In addition to the 60 nm gold nanoparticle suspension from NIST, a silver nanoparticle suspension, nominal diameter 80 nm, was purchased from NanoComposix (USA) for the purposes of confirming the accuracy of the measured transport efficiency. The stock particle suspension was supplied in an aqueous matrix with a 2 mM phosphate buffer. Concentrations of the stock dispersions were reported as 1000mg/L Ag (BioPure product from NanoComposix). Transmission electron micrographs (JEOL 1010 TEM) provided by the manufacturer show near-spherical geometry for the particles. In addition, differential centrifugal sedimentation (DCS) measurements were made in-house to verify average particle diameter and size distribution (CPS Instruments, Florida). For the DCS measurements, the silver nanoparticles were diluted to 20mg/L Ag, and for spICP-MS analysis, the nanoparticle stock dispersions were diluted to concentrations ranging from 0.005 to 0.1μg/L Ag. Triplicate dilutions, of both gold and silver nanoparticles, were freshly prepared daily prior to ICP-MS analysis to minimize particle dissolution and/or aggregation in the samples. All dilutions were made in MilliQ water (18.2 MΩ, filtered through 0.22 μm).

RESULTS AND DISCUSSION

Comparison of measured transport efficiencies

The main aim of this study was to describe the necessary steps to count and size metal-containing nanoparticles using spICP-MS. A crucial part of this objective was developing and assessing methods for determining transport efficiency that are both easy and accurate. Three different methods for measuring transport efficiency were explored. Table 2 shows the efficiencies found by the different methods during three different runs. For each run the particle frequency and particle size methods produced similar efficiencies, while the waste collection method was consistently around 50% higher. When applied to the counting and sizing of a silver nanoparticle sample this discrepancy in the transport efficiency inevitably lead to different calculated particle number concentrations and particle size distributions. Figure 2 shows the resulting particle number concentrations of the silver nanoparticle

sample for different total silver concentrations calculated using the three different measured efficiency values. For comparison, the expected particle number concentration plotted as a function of total silver concentration is shown as a solid line, which is a theoretical calculation based on an average particle size of 72.8±0.4 nm diameter (determined by the peak intensity from three replicate DCS measurements). The expected particle number concentrations overlapped closely with the measured particle number concentrations that were calculated using the transport efficiency determined by either of the two novel methods presented above. Conversely, the efficiency value from the waste collection method consistently underestimated particle number concentration, suggesting an overestimation of transport efficiency.

This overestimation of transport efficiency by the waste collection method was further confirmed when calculating particle size. Figure 3 shows the particle size distribution of the silver nanoparticle sample calculated using the three different measured transport efficiency values. For comparison, the particle size distribution as measured by DCS is also shown. Again, the efficiency values from both the particle frequency and particle size methods produced size distributions comparable to the DCS, whereas the higher transport efficiency measured by the waste collection method overestimated particle size. This same trend was observed in the calculated size distribution over all three analysis runs (Figure S-1, Supporting Information).

The tendency of indirect methods to overestimate efficiency has been shown previously[28] and is attributed to the sensitivity of indirect methods to small recovery losses. Because of this tendency, efforts were made to reduce these losses. For instance, the spray chamber was cooled to 4°C to reduce losses from water vapor and the introduction systems were flushed with air to remove residual liquid in the spray chamber dead space. However, despite these efforts, the waste collection method used in this study consistently overestimated transport efficiency.

Advantages of using transport efficiency to find particle size

Transport efficiency was introduced initially as an important term in the calculation of particle number concentration by Degueldre et al.[14]. The present study introduces a new protocol, which also applies transport efficiency to the calculation of particle size. This protocol is unique from the previously described method in that it does not depend on monodisperse nanoparticles of the same composition as the unknown sample to find size. This ultimately reduces the complexity, and potentially the cost, of characterizing multiple nanoparticle types by spICP-MS by reducing the number of reference nanoparticles required. In this study a gold reference nanoparticle was used to count and size a silver nanoparticle sample, but this same gold reference nanoparticle and protocol could be further extended to characterize a variety of other metal-containing nanoparticles.

spICP-MS as a new tool for nanoparticle characterization

As a counting and sizing technique, the main advantage of spICP-MS over other techniques is its high sensitivity. The samples in the present study were all diluted to below 1 μg/L, and both size and particle number data were accurately obtained at these concentrations (see Figures 2 and 3). Another advantage of spICP-MS is the ability of the technique to better discriminate, based on elemental composition, the nanoparticle of interest from other incidental and/or natural particles, whereas many current counting and sizing techniques are unable to distinguish different types of particulates. However, additional segregation by other methods before spICP-MS analysis will still be necessary to further differentiate particles with the same elemental component as the target nanoparticle (i.e. Ag versus AgS nanoparticles). From a practical viewpoint, spICP-MS utilizes a reasonably common

laboratory instrument in a typical ICP-MS laboratory, and requires little in the way of additional specialized equipment. Furthermore, spICP-MS analysis is technically very similar to traditional ICP-MS analysis, which means the training and expertise of an ICP-MS operator would easily translate to spICP-MS.

While spICP-MS offers many benefits, there are also still many challenges to overcome. For instance, the ability of spICP-MS to determine nanoparticle size relies on two key assumptions, the first being that the particle composition is known and the second being that the particle geometry is known. In controlled laboratory studies, where there is a-priori knowledge of what nanoparticles are in the system, these assumptions are more easily made. However, for environmental samples it becomes difficult to connect a pulse detected by spICP-MS to one particular nanoparticle type and shape. This is especially true for ICP-MS instruments with quadrapole mass analyzers (one of the most popular types), since they are limited to single isotope monitoring of the nanoparticle samples. Another major hurdle with spICP-MS is improvement of the size detection limit. For purposes of method development this study presents an ideal scenario in that the dissolved background was near blank levels and the target nanoparticle consisted of a single element that exhibits high instrument sensitivities. For multi-element particles and less ideal systems, spICP-MS may struggle to detect and size particles within the nano-scale range. Ultimately, improvements to the size detection limit will highly depend on improvements to overall ICP-MS instrument sensitivity.

Further development of this technique will involve additional investigations into the method's various analytical parameters such as dwell time, sample flow rate, etc. In addition, a thorough validation of the technique is needed. This should include assessing the various performance characteristics of the technique, especially in comparison to other commercially available techniques used in the characterization of nanoparticles[25]. Ongoing work is also assessing spICP-MS performance across different instruments and laboratories.

Supplementary Material

Refer to Web version on PubMed Central for supplementary material.

Acknowledgments

This work was conducted at CSIRO Land and Water with funding from the Australian-American Fulbright Scholarship Program. Additional support for this work was also received from the National Institutes of Health Grand Opportunities (RC2) program through National Institute of Environmental Health Sciences grant DE-FG02-08ER64613, the U.S. Army Engineer Research and Development Center Cooperative (Agreement # W912HZ-10-2-026), and the U.S. Environmental Protection Agency- Science to Achieve Results (STAR) Program under grant no. RD-83332401-0. We would like to give special thanks Maxine McCall and Simon Apte from CSIRO for their valuable discussions during this project.

REFERENCES

1. NNI. [accessed July 20, 2010] What is Nanotechnology?. http://ww.nano.gove/html/facts/whatIsnano.html
2. Jang HD, Kim S-K, Kim S-J. J. Nanopart. Res. 2001; 3:141–147.
3. Limbach LK, Li Y, Grass RN, Brunner TJ, Hintermann MA, Muller M, Gunther D, Stark WJ. Environ. Sci. Technol. 2005; 39(23):9370–9376. [PubMed: 16382966]
4. Franklin NM, Rogers NJ, Apte SC, Batley GE, Gadd GE, Casey PS. Environ. Sci. Technol. 2007; 41(24):8484–8490. [PubMed: 18200883]
5. Clift MJD, Rothen-Rutishauser B, Brown DM, Duffin R, Donaldson K, Proudfoot L, Guy K, Stone V. Toxicol. Appl. Pharmacol. 2008; 232(3):418–427. [PubMed: 18708083]

6. Pace HE, Lesher EK, Ranville JF. Environ. Toxicol. Chem. 2010; 29(6):1338–1344. [PubMed: 20821577]
7. Christian P, Von der Kammer F, Baalousha M, Hofmann T. Ecotoxicology. 2008; 17(5):326–343. [PubMed: 18459043]
8. Hassellöv M, Readman J, Ranville JF, Tiede K. Ecotoxicology. 2008; 17(5):344–361. [PubMed: 18483764]
9. Tiede K, Boxall A, Tear S, Lewis J, David H, Hassellöv M. Food Addit. Contam. 2008; 25(7):795–821.
10. Boxall ABA, Tiede K, Chaudhry Q. Nanomedicine. 2007; 2(6):919–927. [PubMed: 18095854]
11. Gottschalk F, Sonderer T, Scholz RW, Nowack B. Environ. Sci. Technol. 2009; 43(24):9216–9222. [PubMed: 20000512]
12. USEPA. Development, Office of Research and Development, Ed. 2009 Jun. Nanomaterial Research Strategy.
13. Klaine SJ, Alvarez PJJ, Batley GE, Fernandes TF, Handy RD, Lyon DY, Mahendra S, McLaughlin MJ, Lead JR. Environ. Toxicol. Chem. 2008; 27(9):1825–1851. [PubMed: 19086204]
14. Degueldre C, Favarger P, Bitea C. Anal. Chim. Acta. 2004; 518(1–2):137–142.
15. Degueldre C, Favarger P. Colloids Surf., A. 2003; 217(1–3):137–142.
16. Degueldre C, Favarger P. Talanta. 2004; 62(5):1051–1054. [PubMed: 18969397]
17. Degueldre C, Favarger P, Wold S. Anal. Chim. Acta. 2006; 555(2):263–268.
18. Degueldre C, Favarger P, Rossé R, Wold S. Talanta. 2006; 68(3):623–628. [PubMed: 18970366]
19. Laborda F, Jimenez-Lamana J, Bolea E, Castillo JR. J. Anal. At. Spectrom. 2011
20. Hu S, Liu R, Zhang S, Huang Z, Xing Z, Zhang X. J. Am. Soc. Mass Spectrom. 2009; 20(6):1096–1103. [PubMed: 19446784]
21. Garcia CC, Murtazin A, Groh S, Horvatic V, Niemax K. J. Anal. At. Spectrom. 2010; 25(5):645–653.
22. Ho K-S, Chan W-T. J. Anal. Atom. Spectrom. 2010; 25(7):1114–1122.
23. Yau MHP, Chan W-T. J. Anal. Atom. Spectrom. 2005; 20(11):1197–1202.
24. Mitrano DM, Lesher EK, Bednar A, Monserud J, Higgins CP, Ranville JF. Environ. Toxicol. Chem. **In press**.
25. Pace HE, Rogers NJ, Jarolimek C, Coleman VA, Higgins CP, Ranville JF. Environ. Sci. Technol. **Submitted**.
26. Montaser, A. Inductively coupled plasma mass spectrometry. New York: Wiley-VCH; 1998.
27. Kato K. Fresenius' J. Anal. Chem. 1988; 329(8):861–863.
28. Smith DD, Browner RF. Anal. Chem. 1982; 54(3):533–537.
29. Van Borm WAH, AC Broekaert J, Klockenkämper R, Tschöpel P, adams FC. Spectrochim. Acta, Part B. 1991; 46(6–7):1033–1049.
30. Todoli, J-L.; Mermet, J-M. Liquid sample introduction in ICP spectrometry: A practical guide. Amsterdam, The Netherlands: Elsevier; 2008.
31. Olesik JW, Kinzer JA, Harkleroad B. Anal. Chem. 1994; 66(13):2022–2030.
32. Farino J, Miller JR, Smith DD, Browner RF. Anal. Chem. 1987; 59(18):2303–2309.
33. Ebdon L, Foulkes M, Sutton K. J. Anal. Atom. Spectrom. 1997; 12(2):213–229.
34. Santos MC, Nóbrega JA. Appl. Spectrosc. Rev. 2006; 41(4):427–448.
35. Ebdon L, Collier AR. Spectrochim. Acta, Part B. 1988; 43(4–5):355–369.
36. Ebdon L, Foulkes ME, Hill S. J. Anal. Atom. Spectrom. 1990; 5(1):67–73.
37. Goodall P, Foulkes ME, Ebdon L. Spectrochim. Acta, Part B. 1993; 48(13):1563–1577.
38. Mochizuki T, Sakashita A, Iwata H, Ishibashi Y, Gunji N. Fresenius' J. Anal. Chem. 1991; 339(12):889–894.
39. Olson KW, Haas WJ, Fassel VA. Anal. Chem. 1977; 49(4):632–637.
40. Gustavsson A. Spectrochim. Acta, Part B. 1984; 39(5):743–746.
41. [accessed July 1, 2011] NIST Reference Material 8013, Gold Nanoparticles nominal 60nm diameter Report of Investigation. https://www-s.nist.gov/srmors/view_report.cfm?srm=8013

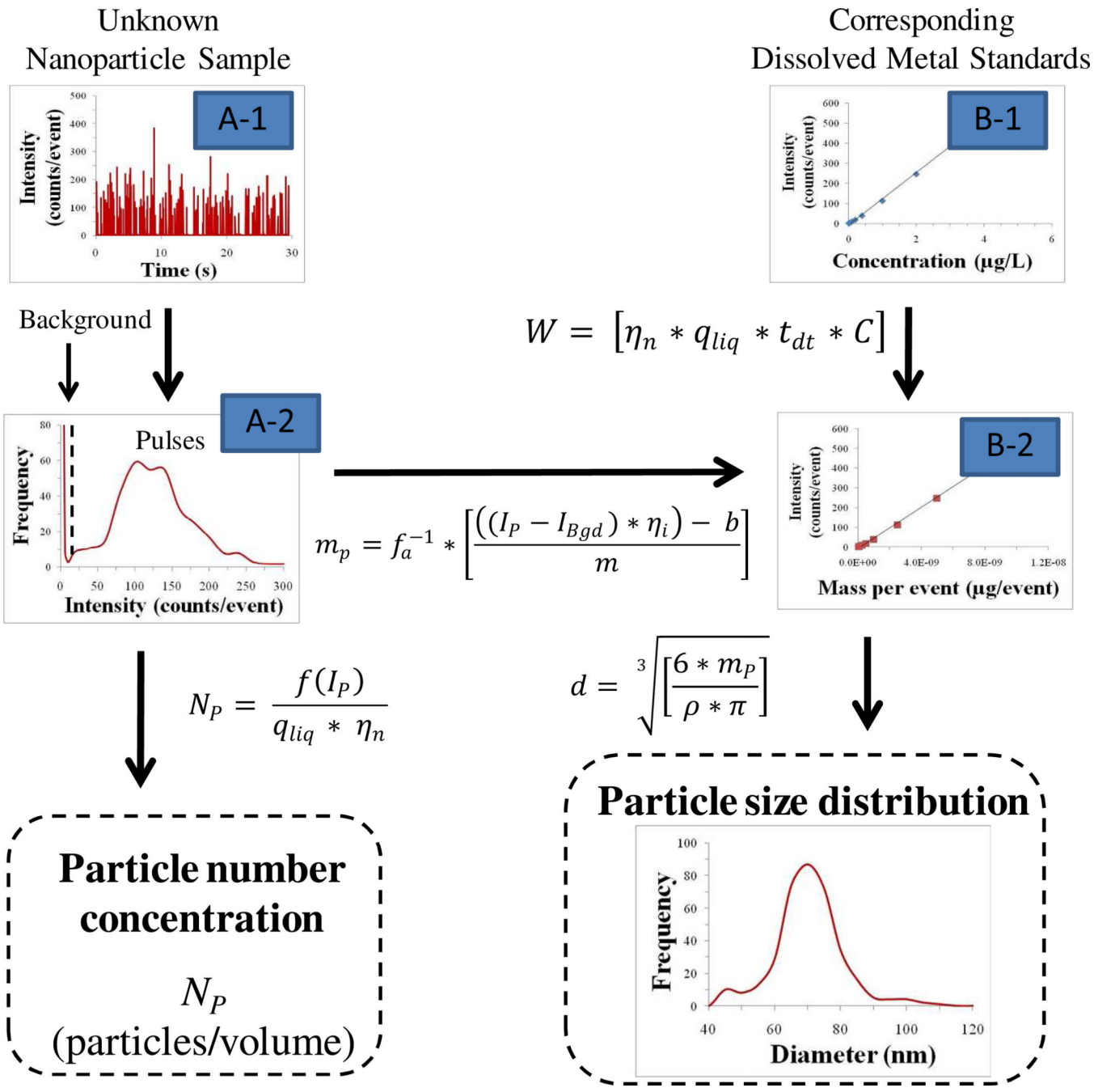

Figure 1.

Data processing schematic for counting (Path A) and sizing (Path A & B) nanoparticles using single particle ICP-MS. **A-1** Raw data of unknown sample, **A-2** Sorted and binned raw data to separate pulses from the background, **B-1** Calibration curve of dissolved standards created for particle size calculation, **B-2** Transformed calibration curve from concentration to mass per event. Particle number concentration is determined by dividing the frequency of pulse events ($f(I_p)$) by the sample flow rate (q_{liq}) times the transport efficiency (η_n). Particle mass (m_p) is calculated by inserting individual pulse intensities (I_p), minus the average background intensity (I_{Bgd}), into the transformed calibration curve (y=mx + b). If

applicable, ionization efficiency (η_i) and the mass fraction (f_a^{-1}) of the particle are included. Convert particle mass to particle diameter and bin data to create a particle size distribution.

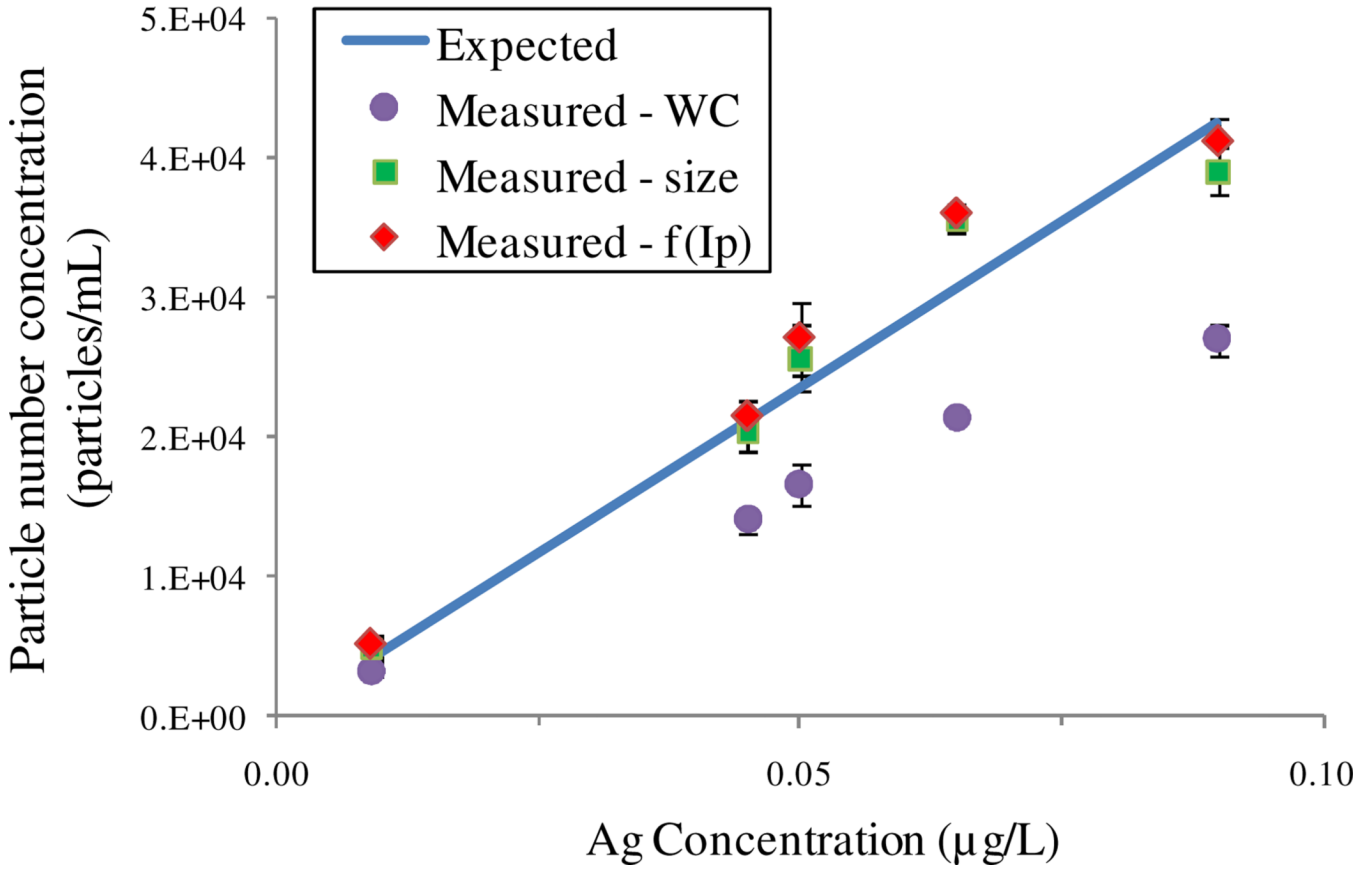

Figure 2.
Particle number concentrations of silver nanoparticle samples, analyzed by single particle ICP-MS, using three different measured transport efficiencies (WC = waste collection method, size = particle size method, f(Ip) = particle frequency method). Expected particle number concentrations calculated using average particle size and total silver concentration.

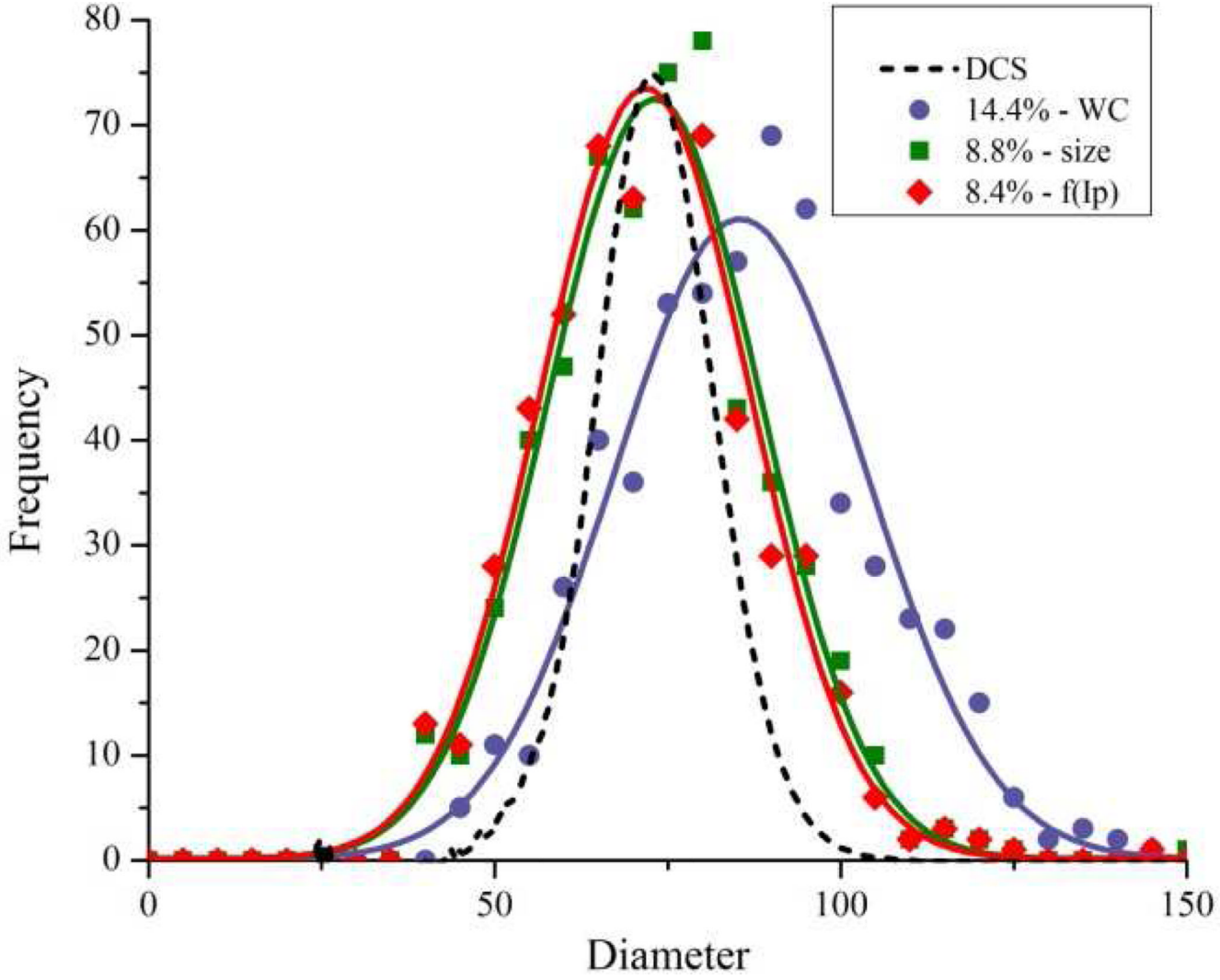

Figure 3.
Particle size distribution of a silver nanoparticle suspension, analyzed by single particle ICP-MS, using three different measured transport efficiencies (WC = waste collection method in purple, size = particle size method in green, and f(Ip) = particle frequency method in orange). Size distribution from differential centrifugal sedimentation (DCS) analysis is shown for comparison.

Table 1

Overview of three methods for measuring transport efficiency (η_n)

	Method 1 **Waste collection**[1]	**Method 2** **Particle size**	**Method 3** **Particle frequency**
Known parameters	Solution volume	Particle size (Reference nanoparticle)[3]	Particle number concentration[2] (Reference nanoparticle)[3]
Measured parameters	Sample flow rate Weight of sample vial with solution plus waste vial and tubing before and after 60+ minutes of aspiration	Sample flow rate Peak intensity[4] Calibration curve for corresponding dissolved reference nanoparticle material	Sample flow rate Pulse frequency
Key equations	$\eta_n = \frac{\Delta \text{total weight}}{\Delta \text{sample weight}}$	$\eta_n = \frac{m_{diss}}{m_{NP}}$	$\eta_n = \frac{f(I_p)}{q_{lia} * N_P}$

[1] Waste collection method adapted from Gustavsson[40]

[2] Particle number concentration is calculated from the average particle size and total metal concentration of the reference nanoparticle suspension in the present study

[3] Reference nanoparticle used for this study was the US National Institute of Standards and Technology Reference Material RM8013 (gold nanoparticle with a nominal diameter of 60nm)

[4] Peak intensity is found by fitting a curve to the histogrammed raw data from the spICP-MS analysis of a reference nanoparticle

Table 2

Comparison of the measured transport efficiencies by three different methods

	Method 1	Method 2	Method 3
Replicate	**Waste collection**	**Particle size**	**Particle frequency**
Day 1 (12/1/10)	-[a]	9.1±0.2%	9.0±0.9%
Day 2 (12/22/10)	14.4±1.2%	8.8±0.4%	8.4±1.1%
Day 3 (1/12/11)	14.5±0.7%	8.6±0.2%	8.7±0.7%

[a]Measurement not reported due to sampling error